UNIDIRECTIONAL SODIUM AND POTASSIUM FLUXES THROUGH THE SODIUM CHANNEL OF SQUID GIANT AXONS

DAVID BUSATH AND TED BEGENISICH
Department of Physiology, University of Rochester School of Medicine, Rochester, New York 14642

ABSTRACT Unidirectional ^{22}Na-traced sodium influx or ^{42}K-traced potassium efflux across the membranes of voltage-clamped squid giant axons was measured at various membrane potentials under bi-ionic conditions. Tetrodotoxin almost entirely eliminated the extra K^+ efflux induced by short repetitive depolarizations in the presence of tetraethylammonium or 3,4-diaminopyridine. A method of determining the voltage dependence of the unidirectional flux through voltage-gated channels is described. This technique was used to obtain the unidirectional flux-voltage relation for the sodium channel in bi-ionic and single-ion conditions. It allows the determination of the unidirectional flux at the zero-current potential which, for influx, was found to be ~20% of the value measured 80 mV negative to the zero-current potential. The unidirectional flux ratio under bi-ionic conditions was also measured and the flux ratio exponent found to average 1.15 with an external sodium solution and an internal potassium solution. A three-barrier, two-site, multi-occupancy model previously obtained for other conditions was found to predict a similar non-unity average for the flux ratio exponent. It is also shown that some single-occupancy models can predict non-unity values for the flux ratio exponent in bi-ionic conditions.

INTRODUCTION

Most studies of the ionic permeation processes of the sodium and potassium channels in nerve have employed measurements of ionic currents and zero current potentials (Hille, 1975; Begenisich and Cahalan, 1980 *a*, *b*). The results of these studies have shown that the sodium channel of squid giant axons behaves under some conditions like a multi-ion pore. A particular permeation model has been presented which can account for most of the electrical measurements (Begenisich and Cahalan, 1980 *a*, *b*).

It is possible to study the unidirectional ionic fluxes as well as currents in giant axons. We have already reported measurements of the ratio of the unidirectional influxes and effluxes of sodium ions through the sodium channel of these nerve fibers (Begenisich and Busath, 1981). In the present study we measure ^{22}Na influx and ^{42}K efflux in fibers bathed in K-free seawater and perfused with Na-free internal solutions. We describe a method of determining the voltage dependence of the individual unidirectional ionic fluxes. We apply this technique to axons with both K-free and Na-free internal solutions. We also determine the ratio of unidirectional K efflux and Na influx and discuss the significance of the measurement of flux ratios under bi-ionic conditions. Lastly, the predictions of the fluxes from the three-barrier, two-site model determined from electrical measurements are compared with the present results.

METHODS

The methods used in this study have been described previously (Begenisich and Busath, 1981; Begenisich and De Weer, 1980). These experiments were performed at 10°C on well-cleaned giant axons of *Loligo pealei* obtained from the Arrive Alive Biological Supply Company, Long Island, NY. Both live and decapitated animals were used. The diameters of the 25 axons used in this study ranged from 400 to 700 μm, with an average near 500 μm. The resting potential of axons bathed in artificial seawater and internally perfused with KSIS (potassium standard internal solution, see below) averaged −63 mV. The internal perfusion and voltage-clamp techniques were similar to those used by Begenisich and Lynch (1974).

Levis (1981) has described a method for improving series resistance compensation by matching the phases of the membrane voltage and series resistance compensation signals. We have used a simplified version of this technique. An additional benefit of this improvement is a decrease in clamp settling time. Fig. 1 shows the capacitative transient from a typical axon produced by a −30-mV pulse. The transient is essentially complete within 10 μs. In several axons this could be reduced to 8 μs. The decrease in settling time and the improved series resistance compensation provide a more reliable measure of the tail currents used to determine the instantaneous current-voltage relations described below. The series resistance compensation used ranged from 2 to 6 $\Omega \cdot cm^2$ but was usually 4–5 $\Omega \cdot cm^2$ with an average value of 4.3 $\Omega \cdot cm^2$. This average value compares favorably with other measurements of the total (preparation plus electrode) measured series resistance of 3.03 $\Omega \cdot cm^2$ (Binstock et al., 1975) and 4.02 $\Omega \cdot cm^2$ (Salzberg et al., 1981; B. Salzberg, personal communication).

Membrane voltages have been corrected for the junction potential between the 0.56 M KCl internal electrode and the internal perfusion

Dr. Busath's present address is Department of Physiology and Biophysics, University of Texas Medical Branch, Galveston, TX 77550.

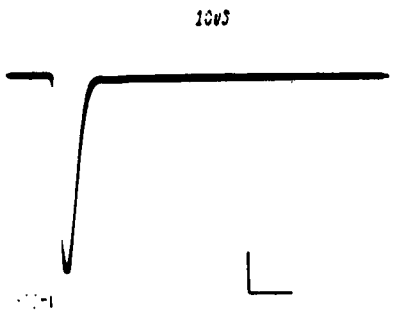

FIGURE 1 The capacitative current transient recorded during a 40-mV hyperpolarization from the holding potential, −80 mV. Several traces were needed to expose the rather slow film used. The vertical and horizontal calibration bars represent 5 mA/cm^2 and 10 μs, respectively.

solutions. The external reference potential was measured with a saturated KCl agar-filled electrode.

Two artificial seawater (ASW) solutions were used. Most of the experiments used a Mg containing ASW consisting of (mM) 400 NaCl; 50 $MgCl_2$; 10 $CaCl_2$; 5 *N*-2-hydroxyethylpiperazine-*N*'-2-ethane sulfonic acid (HEPES) buffer, (pH 7.4–7.6; 950–970 mosmol/kg). In some experiments the Mg was replaced by 140 mM glycine to reduce divalent cation block of sodium channels (Woodhull, 1973; Taylor et al., 1976). This solution is called 0-Mg ASW and was used unless otherwise indicated. Potassium channel currents were blocked either by addition to the internal KSIS solution of 1 mM 3,4-diaminopyridine (Kirsch and Narahashi, 1978) or by addition of 25 mM tetraethylammonium (Armstrong, 1969) and reduction of glycine to 350 mM. The internal perfusion solutions KSIS, Na/Cs SIS and Na/TMA SIS were the same as in Begenisich and Busath (1981). Table I gives their compositions in millimoles per liter.

Only one unidirectional tracer flux (^{22}Na or ^{42}K) was measured in any given experiment. The remaining unidirectional flux was computed from the integral of sodium channel current (net flux) and the measured tracer flux. The controls for the validity of this approach are described in Begenisich and Busath (1981) and Begenisich and De Weer (1980). For most of the membrane potentials used here, the influx and net flux are of comparable magnitudes. Therefore the calculation of efflux as the difference between these two numbers is sensitive to small errors in their measurement. To improve the accuracy of computed efflux, a calibration voltage was used. This value of membrane potential was sufficiently negative that efflux made a negligible contribution to net flux. We therefore determined the ratio of net flux to influx at this potential (called the scale factor) and multiplied the influxes measured at other voltages by this value. The scale factor for influx experiments with Na/Cs and Na/TMA SIS averaged 1.06 and for KSIS averaged 1.16. An analogous calibration can be performed for efflux but this requires using a membrane potential value at least 75 mV more positive than the reversal potential or ~125 mV. Repetitive stimulation at high rates to such large voltages is deleterious to axons. In two axons we measured ^{42}K efflux into a Na-free (Tris replacement) ASW with 25 mM K at voltages near 50 mV. These voltages were substantially more positive than the expected reversal potential, ~−65 mV in this case. Scale factor values of 1.13 and 1.5 were found. Except for the value of 1.5, all values obtained were near unity. The similarities between the results for the influx and efflux techniques shown in Figs. 5 and 7 argue for the validity of this scaling procedure.

TABLE I
INTERNAL SOLUTIONS

Solution	Na	K	TMA	Cs	F	Glutamate	Glycine	Phosphate
K SIS	—	350	—	—	50	270	390	15
200 Na SIS	200	—	—	—	100	50	690	25
Na/Cs SIS	50	—	—	150	150	—	690	25
Na/TMA SIS	50	—	150	—	150	—	690	25

The relationship between the voltage and unidirectional flux through an open channel cannot be measured directly because the average number of channels conducting during the pulse varies from one voltage to another. Rather, we can only measure time-integrated unidirectional flux per pulse, M_e and M_i. However, a measure of open-channel flux can be computed by solving two simultaneous equations. First, for a given voltage, the so-called instantaneous membrane current, I', is proportional to the difference of the open-channel fluxes, m_i and m_e. Second, the ratio of the measurable unidirectional fluxes, M_e/M_i, equals the ratio of the open-channel fluxes.

$$I' = N\,(m_i - m_e) \tag{1}$$

$$M_e/M_i = m_e/m_i \tag{2}$$

I' is measured by opening a fixed, unknown number of channels, N, with a constant prepulse and then measuring the current immediately after test pulses to different voltages, V_m. By measuring I' and M_e/M_i we can solve Eqs. 1 and 2 for m_e and m_i to within the unknown constant, N:

$$N \cdot m_i = \frac{I'}{(1 - M_e/M_i)}; \tag{3}$$

$$N \cdot m_e = \frac{I'}{(M_i/M_e - 1)}. \tag{4}$$

We define these computed values of $N \cdot m_e$ and $N \cdot m_i$ as "instantaneous flux" in analogy with the frequently used term "instantaneous current."

To obtain the instantaneous current-voltage relation, the membrane potential was first stepped from the holding potential to +20 mV for 500 μs in order to open a set of sodium channels. The potential was then stepped to a test value and the membrane current measured at 5- or 10-μs intervals. By repeating the procedure in 1 μM TTX, the amount of nonsodium channel current could also be determined. The TTX-corrected current was extrapolated back to the start of the test pulse by least-squares fitting a single exponential to all but the first 2 of the 8–10 points immediately following the step to the test potential. The zero-time current flowing through the set of open channels was then the instantaneous current for that voltage. The current during the prepulse served as a control for slight changes in temperature.

RESULTS

Instantaneous Flux, Bi-ionic Conditions

The efflux of tracer-labeled potassium from giant axons perfused with KSIS is shown in Fig. 2. In the upper part of the figure, the axon is initially held at −80 mV. The flux increases during periods of repetitive depolarizations to −10 mV, then 110 mV, and finally 30 mV. Corresponding current records are presented in the inset. Because the membrane potential affects both the sodium channel current and the gating kinetics, the measured flux per depolarization at a given voltage reflects the time course of the number of channels open as well as the open channel flux. The effects can be separated by the method for calculating the instantaneous flux outlined above.

In the lower part of Fig. 2, the axon is depolarized

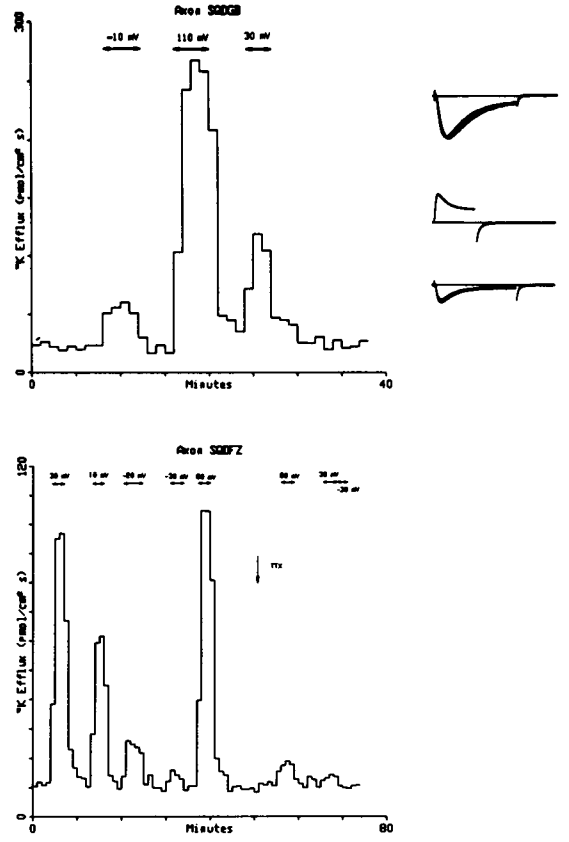

FIGURE 2 Top: potassium efflux from an axon with a holding potential of −80 mV. During the periods marked by arrows, depolarization to the indicated voltage (each preceeded by a 40-ms hyperpolarization to −100 mV) were applied 10 times per second. Inset: sodium currents recorded during the stimulation periods. Currents obtained in TTX ASW have been subtracted. The three sets of records contain currents during depolarizations to −10 (top), 110 (middle), and 30 mV (bottom) lasting 4, 2, and 4 ms, respectively. The peak inward current in the top trace is −3.8 mA/cm^2. Bottom: potassium efflux from an axon held at −80 mV and depolarized 10 times per second to the voltages indicated. At the arrow, ASW containing 1 μM TTX was infused rapidly into the chamber.

repetitively to +30, +10, −20, −30, and +80 mV. Then TTX (1 μM) is added externally and the depolarizations to +80, +30, and −30 mV are repeated. There is a slight increase above the baseline flux during the period of 80-mV pulses and no consistent change from the irregular baseline level during the pulses to +30 and −30 mV. The small TTX-insensitive extra flux during the largest depolarization represents a negligible fraction of the TTX-sensitive extra flux.

The data for experiments on the efflux of ^{42}K in ASW are given in Table II. Column 1 gives in millivolts the voltage (V_m) to which the membrane potential was repetitively stepped. Column 2 contains V_m - V_{rev}, V_{rev} being the peak sodium current reversal potential measured on the same axon. The axon in Fig. 2, SQDGB, had a reversal potential of +54 mV, for example. Column 3 gives the extra tracer flux per pulse. For SQDGB, the depolarizations to −10 mV produced an extra ^{42}K efflux of 3.44 pmol/cm^2·pulse. The integral of the current record divided

TABLE II
^{42}K EFFLUX

Axon influx	V_m	$V_m - V_{rev}$	^{42}K efflux	Net flux	Scale factor	Na influx
	mV	*mV*	*pmol/cm²*	*pmol/cm²*		*pmol/cm²*
SQDFY	−10	−64	1.27	−39.3	NS	40.6
	30	−24	4.81	−26.2		31.0
	40	−14	5.48	− 5.10		10.6
	10	−44	3.58	−31.7		35.3
	20	−34	5.22	−21.4		26.6
SQDFZ	30	−25	8.70	−16.2	NS	24.9
	10	−45	5.14	−30.9		36.0
	−20	−75	1.56	−30.7		32.3
	−30	−85	0.53	−18.1		18.6
	80	25	9.57	7.6		1.97
SQDGA	−10	−75	2.38	−63.8	1.50	67.4
	90	25	12.7	13.9		5.15
	50	−15	6.45	−10.0		19.7
	20	−45	5.00	−44.6		52.1
SQDGB	−10	−64	3.44	−72.0	1.13	75.9
	110	56	25.8	30.3		−1.15
	30	−24	9.87	−21.8		32.3

by Faraday's constant gives a net inward flux of 72 pmol/cm^2·pulse. This is shown in column 4. Column 5 shows the scale factor (where obtained) which, for this case, was 1.13. The sodium influx per pulse is calculated as

$$M_i = \mathrm{SF} \times M_e - M_{net}$$

$$M_i = 1.13 \times 3.44 \text{ pmol/cm}^2 - (-72 \text{ pmol/cm}^2)$$

$$M_i = 75.9 \text{ pmol/cm}^2.$$

This result is contained in column 6. In this axon the net outward flux for the depolarization to 110 mV in SQDGB exceeded the efflux, even when the efflux is modified by the scale factor. This result is not physically reasonable and is no doubt the consequence of small errors in measuring flux. For example, if the K efflux were higher by 5%, the corrected efflux would have exceeded the net flux yielding a (real) Na influx.

Fig. 3 shows an example of the reciprocal experiment: the influx of ^{22}Na from ASW into KSIS perfusate. As in the experiments in Fig. 2, the extra tracer flux during the stimulation periods rapidly achieves a steady level. The addition of TTX abolished the extra influx, though the baseline flux increases rapidly after the 40-mV stimulation period ended, consistent with an increase in nonspecific leakage current. Table III contains these data and the analogous information from other axons where the influx of ^{22}Na into KSIS was measured and the potassium efflux through the sodium channel calculated in a similar fashion.

The instantaneous current-voltage relationships for two axons in (0-Mg) ASW are plotted as triangles in Fig. 4. A polynomial was fit to these data and is plotted as a solid line to provide a visual reference and to allow for interpolation

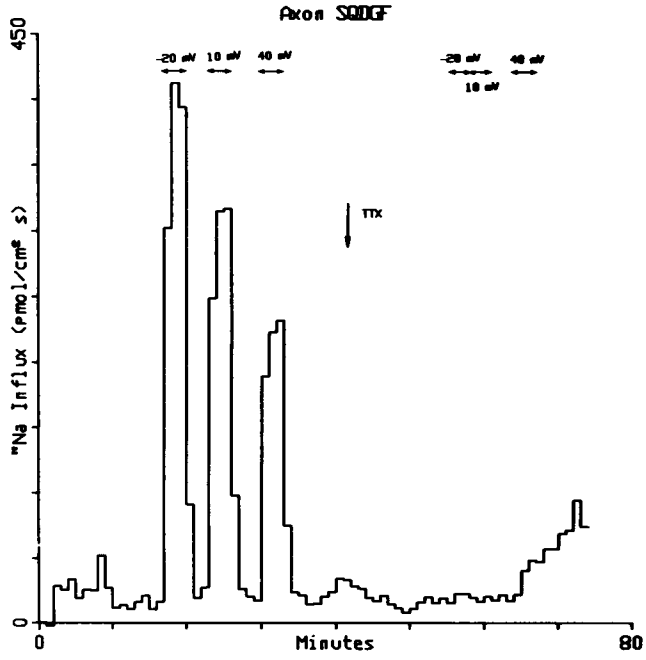

FIGURE 3 Sodium influx into an axon perfused with (sodium-free) KSIS. The membrane potential was held at −80 mV and depolarized 10 times per second to the voltages indicated during periods marked by arrows. 1 μM TTX ASW was infused at the time indicated by the arrow.

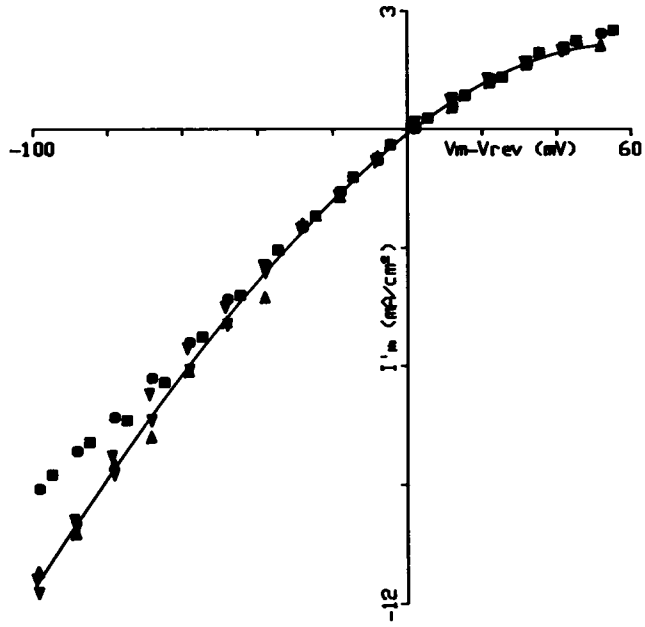

FIGURE 4 The instantaneous current plotted against driving force for two axons perfused with KSIS internally and bathed in 50-Mg^{++} ASW and 0-Mg^{++} ASW. In the order listed in the inset, the currents were scaled by factors of 1.34, 3.77, 1.0, and 7.05. Reversal potentia ls were 60, 56, 60, and 60 mV. The solid line is a polynomial fit to the 0-Mg^{++} ASW data. The similarity in the shape of the *I-V* between axon SQDGH and SQDGI in 0-Mg^{++} ASW when the current density in SQDGI was sevenfold lower indicates that series resistance errors are negligible. For 50-Mg^{++} ASW, ●, axon SQDGH; ■, axon SQDGI. For 0-Mg^{++}, ▼, axon SQDGH; ▲, axon SQDGI.

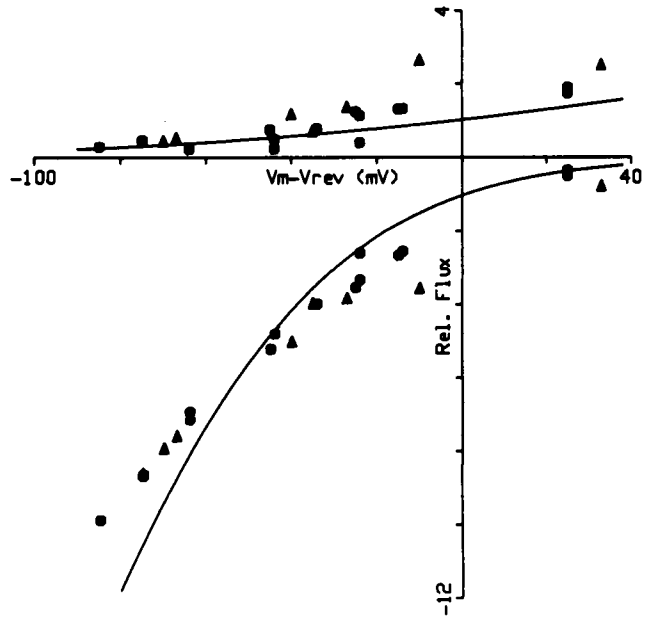

FIGURE 5 Instantaneous potassium efflux and calculated instantaneous sodium influx (●) or calcuated instantaneous potassium efflux and instantaneous sodium influx (▲) plotted against driving force using the flux data in Tables II and III and the instantaneous current interpolated from Fig. 4. Because axon SQDGH was the standard for Fig. 4, the flux is relative to axon SQDGH. For the points from axon SQDGH, the instantaneous flux in millimoles per square centimeter per second can be obtained by dividing the relative flux in the plot by the Faraday constant. Sodium influx is plotted as negative and potassium efflux as positive. V_{rev} averaged 54 mV (SD = 6 mV, n = 7).

between voltages. Also plotted are measurements made on the same axons but in the presence of 50 mM Mg^{++}. At negative voltages, these points lie substantially above the curve due to voltage-dependent, divalent cation block (Woodhull, 1973; Taylor et al., 1976).

The instantaneous flux calculated using Eqs. 3 and 4 is plotted against V_m - V_{rev} in Fig. 5. The instantaneous fluxes in Fig. 5 are normalized with respect to axon SQDGH. The ordinate in the figure is given as relative flux. Data from efflux experiments in Table III are plotted as circles. Those

TABLE III
^{22}Na INFLUX

Axon	V_m	$V_m - V_{rev}$	^{22}Na influx	Net flux	Scale factor	K efflux
	mV	*mV*	*pmol/cm²*	*pmol/cm²*		*pmol/cm²*
SQDGE	10	−35	4.41	−4.01	1.10	0.84
	−30	−75	12.6	−13.2		0.66
SQDGF	−20	−70	38.3	37.0	1.02	2.07
	10	−40	29.6	23.3		6.89
	40	−10	20.7	5.60		15.5
SQDGG	−12	−67	11.9	−15.1	1.36	1.07
	28	−27	7.67	−6.77		3.66
	88	33	4.24*	12.1		17.9

*Corrected for tail influx.

from the influx experiments are shown as triangles. Potassium efflux through the sodium channel is plotted as positive values and Na influx as negative. By comparing the triangles with the circles, it can be seen that, for both influx and efflux, the calculated values fit well with the directly measured values. Since the calculated values have been scaled using the calibration pulse method, this observation shows that the scaling procedure is reasonable. The sum of the two curves gives the instantaneous current-voltage relationship. At $V_m = V_{rev}$, though no net current flows, there continue to flow opposite but equal one-way fluxes of a magnitude corresponding to ~20% of the influx at −80 mV from V_{rev}. The solid curves plotted are the predictions from the three-barrier, two-site model described previously (Begenisich and Cahalan, 1980 *a*, *b*). Although the model does not provide an adequate quantitative prediction of the measured influx, it does give a good fit to other data previously reported (Begenisich and Cahalan, 1980 *a*, *b*; Begenisich and Busath, 1981) and other data in this paper. Possible reasons for the discrepancy will be considered in the Discussion.

Instantaneous Flux, Single-Ion Conditions

Since unidirectional and net flux-per-pulse measurements had been made previously with Na/Cs SIS and Na/TMA SIS (Begenisich and Busath, 1981) instantaneous fluxes with Na as the only permeant ion can be computed using the appropriate instantaneous current-voltage relationship. The current-voltage curves obtained with Na/Cs SIS (with and without 50 mM Mg^{++} in the external solution) are shown in Fig. 6, together with a plot of the polynomial fit to the 0-Mg^{++} ASW data. Again we calculated the instantaneous fluxes according to Eqs. 3 and 4 and these are plotted in Fig. 7. Both the influx and efflux methods yield similar results. The instantaneous flux extrapolated to the reversal potential is again ~20% of the influx at −80 mV from V_{rev} as in the bi-ionic case. The solid curves have been calculated using the three-barrier, two-site model.

Flux Ratio in Bi-ionic Conditions

Theoretical considerations of the flux ratio in the past have focused on expectations for a single type of permeant ion. Nevertheless, inasmuch as we have measured the individual unidirectional fluxes in bi-ionic conditions, it seems appropriate to present the results in the flux ratio format. Some consideration of the expectations for the bi-ionic flux-ratio-voltage relation will be given in the Discussion and Appendix. The ratios of potassium efflux to sodium influx from Table II (efflux method) and Table III (influx method) are plotted semilogarythmically in Fig. 8. The dashed line is a straight line with a slope corresponding to a flux ratio exponent, n' (see Appendix) of unity. The average value of n' for all of the data is 1.15, which is significantly greater than unity ($P < 0.01$). The solid curve

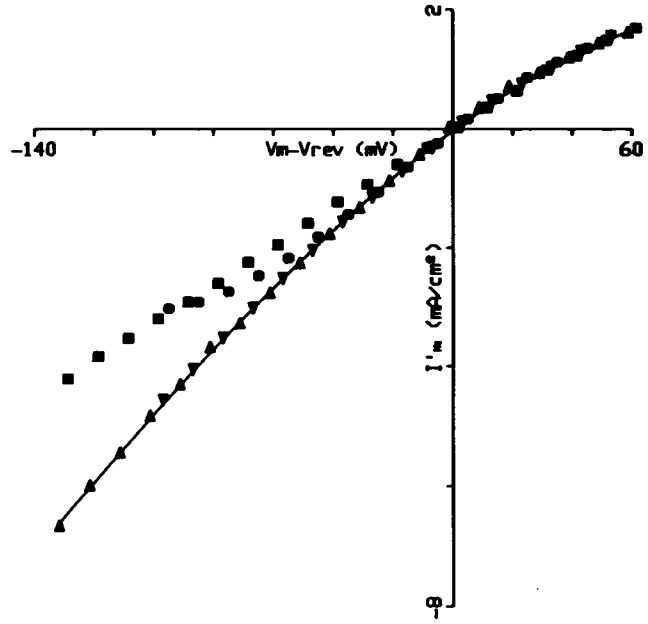

FIGURE 6 Instantaneous current vs. driving force for two axons perfused with Na/Cs SIS and bathed in 50-Mg^{++} and 0-Mg^{++} ASW. No scaling of the currents was used. The reversal potentials were 48 and 50 mV for axon SQDHA in 50-Mg^{++} and 0-Mg^{++} ASW, respectively, and were not obtained for Axon SQDGI. The solid line is a polynomial fit to the 0-Mg^{++} ASW data. For 50-Mg^{++} ASW, ●, axon SQDHA; ■, axon SQDGI. For 0-Mg^{++} ASW, ▼, axon SQDHA; ▲, axon SQDGI.

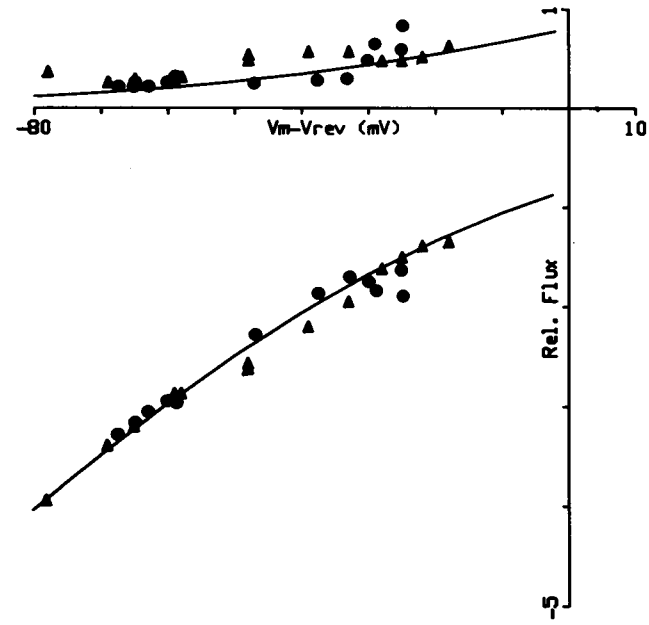

FIGURE 7 Instantaneous flux vs. driving force using Na/Cs and Na/TMA SIS data from Tables II and III (Begenisich and Busath, 1981) and the instantaneous current from Fig. 6. The flux is relative to axons SQDHA and SQDGI. Sodium influx is negative and sodium efflux is positive. As in Fig. 5, triangles in the positive range and circles in the negative range represent calculated flux. V_{rev} averaged 54 mV (SD = 5 mV, n = 13).

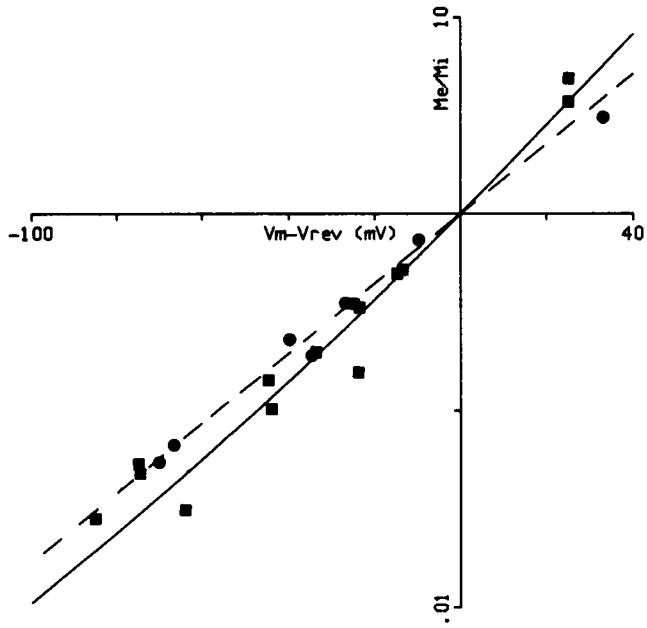

FIGURE 8 The ratio of potassium efflux to calculated sodium influx (■) or calculated potassium efflux to sodium influx (●) plotted logarithmically against driving force. The dashed straight line corresponds to a constant n' with a value of 1.0. The solid curve is the prediction of the three-barrier, two-site model obtained by Begenisich and Cahalan (1980 *a*, *b*).

which appears to fit the data well, has been calculated from the three-barrier, two-site model. The model predicts values for n' between 1.10 and 1.27 over the voltage range displayed.

DISCUSSION

We have shown that it is possible to determine the relationship between open sodium channel flux and voltage. This measurement provides a method of obtaining the relative open channel influx and efflux at the zero-current potential. Also it provides a more fundamental data set than either the flux-ratio or current-voltage relations. Although theoretically there is no information contained in the instantaneous flux curves that is not also contained in the flux-ratio and instantaneous current-voltage curves from which they were derived, displaying the fundamental data set is advantageous in that it represents a less complicated combination of the parameters of the underlying physical process. For instance, for a pore whose transport was limited by a single energy barrier, the effective position of the barrier in the electric field could be determined directly from the steepness of the instantaneous flux curve, whereas the flux-ratio or instantaneous current-voltage curves do not provide that information directly. Furthermore, to predict the instantaneous flux-voltage curve, one less parameter (i.e., the rate of entry of an ion from the side opposite the measured species) is required.

In this paper we have compared the predictions of the model obtained previously by Begenisich and Cahalan (1980 *a*, *b*) to our data. This model resulted from experiments of a different type done in different conditions. Specifically, Begenisich and Cahalan measured sodium channel reversal potentials, instantaneous current-voltage relations, and current-concentration relations for a variety of Na^+, K^+, and NH_4^+ concentrations on both sides of the squid axon membrane. Then they systematically sought out a set of barrier patterns that could predict their measurements. In the fitting, they made two major simplifying assumptions: (*a*) the barrier and well positions were arbitrarily assumed beforehand to be symmetrically placed and the same for all ions, thus fixing the voltage dependence of the rate constants; and (*b*) there was no repulsive interaction between ions in doubly occupied pores. Thus, this model is one of the simplest possible single-filing, multi-occupancy models. The energy barriers for this model are, in RT units from outside to inside, 10.5, 7.5, and 10 for sodium and 11.5, 12.8, and 10.0 for potassium. The well depths chosen were 0 and −0.75 for sodium and 0 and −2.2 for potassium. It is noteworthy that no single barrier predominates.

We feel that the fit of the model to the data presented in this paper is good except for the influx data of Fig. 5. However, we do not wish to imply that the complexity of the multi-occupancy model is necessary to fit these data. Indeed, simpler models such as the integrated Nernst-Planck equation fit the instantaneous fluxes nearly as well over this voltage range. An effort to distinguish between the three-barrier, two-site model and electrodiffusion based on instantaneous flux measurements, given the errors we experience in measuring tracer flux, would require ~75–100 mV more range in voltage. Although models based on electrodiffusion could describe the present data over this limited voltage range, such models cannot account for many other properties of the sodium pore (Begenisich and Cahalan, 1980 *a*, *b*). It is important to emphasize that the parameters of this three-barrier, two-site model were initially selected with the intention of providing a reasonable fit to a wide variety of data. The model predicted a steeper curvature with voltage then was observed for unidirectional flux in bi-ionic conditions (Fig. 5). Nevertheless, the other new data presented here (Fig. 5, efflux, Fig. 7, and Fig. 8) are well described by even this simple model. Although the addition of ionic repulsion to the model or other changes in the parameters may improve the fit to the influx data, we show that this simple model can at least qualitatively describe the measurements we report here.

The introduction of the bi-ionic flux ratio in this paper requires some theoretical consideration. In conditions where a single permeant ion species is present on both sides of the membrane, the relation between the flux ratio and $V_m - V_{rev}$ is predicted by electrodiffusion arguments (Ussing, 1949) to change e-fold every RT/Fz (24.4 mV at 10°C, univalent ions). This relation has been predicted to have a steeper slope for channels where several ions are

restricted to move in file through the membrane (Hodgkin and Keynes, 1955; Heckmann, 1972; Hille and Schwarz, 1978). The increased steepness factor is usually denoted by n'. The bi-ionic flux ratio is the ratio of fluxes of two different species present on opposite sides of the membrane. The steepness factor is unity, even for bi-ionic conditions, for pores where the Goldman-Hodgkin-Katz current equation applies. Also, flux coupling is expected to increase n' above unity as it does in single-ion conditions. However, values of n' different from one in bi-ionic conditions need not be due solely to single-filing.

In the Appendix we demonstrate that n' can be <1 or >1 in bi-ionic conditions due to differences in predominant barrier position. For instance, if the predominant barrier to sodium were near the external channel mouth and the predominant barrier to potassium were near the internal mouth, n' would approach zero. On the other hand, predominance of barriers distal to ion entry would tend to increase n' above unity.

We find a bi-ionic flux ratio for Na ASW//KSIS of 1.15. The distribution of the barrier heights in the Begenisich-Cahalan model is consistent with this result. The extent to which this small deviation from unity is caused by barrier position asymmetry (vs. flux coupling) might be examined by calculating the flux ratio exponent for a pore with identical barrier patterns but with double occupancy disallowed. Deviations from unity for the single-ion pore would then reflect only asymmetry differences. A calculation using the Begenisich-Cahalan barriers, but excluding multiple-occupancy, gives n' between 1.03 and 1.20 for membrane potential between -30 and 100 mV. Therefore in a single-occupancy pore with the Begenisich-Cahalan barriers, the bi-ionic n' exceeds unity due to barrier asymmetry alone. As mentioned above, when multiple occupancy is allowed, the same barriers give n' between 1.10 and 1.27 in this voltage range. The very small increase in n' in the multiple occupancy case is attributable to flux coupling. The model predicts the fraction of doubly occupied channels to be 0.17 and 0.07 at -30 and 100 mV, respectively.

In conclusion, a method of measuring the unidirectional flux-voltage relationship has been used to estimate fluxes of sodium and potassium in the sodium channel of the squid giant axon under bi-ionic and mono-ionic conditions. The ratio of sodium influx to potassium efflux was also calculated at several voltages. The predictions of the simple three-barrier, two-site multi-ion model proposed by Begenisich and Cahalan were consistent with all of these measurements.

APPENDIX

One simple model to consider in attempting to understand the meaning of the bi-ionic n' is the single-barrier model. It is illustrated in the left-hand panel of Fig. 9. On the top, a barrier diagram for ion A is shown and the diagram for ion B is beneath. In both cases, the outside of the cell is to the left of the barrier pattern. Because the two different ions may experience different energy restrictions, they may need to cross peaks of different heights, $G_1^A = G_1^{\dagger A}/RT$ for the external ion and $G_1^B = G_1^{\dagger B}/RT$ for the internal ion, at different fractions α_1^A and α_1^B inward through the membrane field. Let the reduced electrical potential $\psi = FzV_m/RT$, be $\Psi_o = 0$, $\Psi_i = \Psi$. If ion A has activity A on only the outside of the membrane and ion B has activity B on the inside only, Eyring absolute

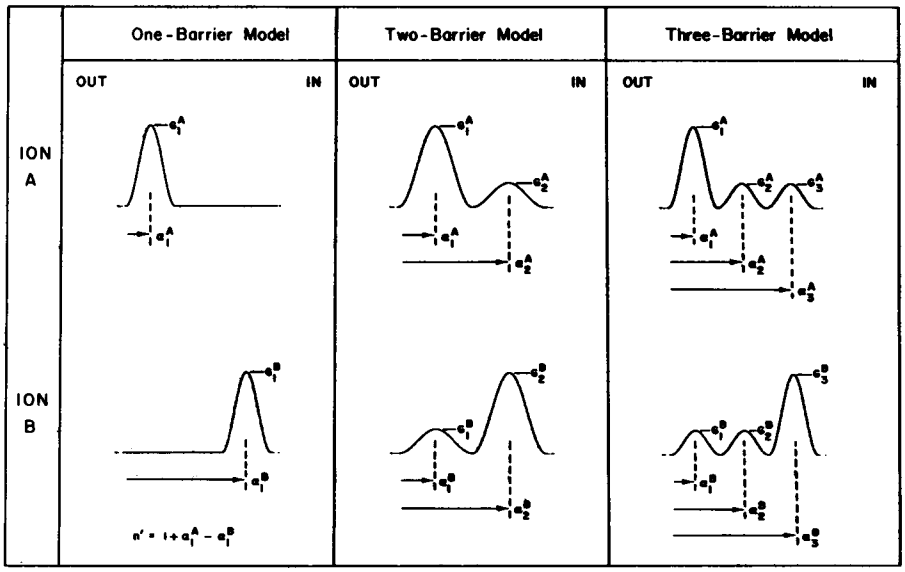

FIGURE 9 Schematic representations of possible potential energy profiles limiting passive ion movement through a membrane channel. For two ion species, A and B, the heights and positions of the barriers (and wells) conceivably could vary. The outside of the membrane is on the left. α is the fractional distance rightward through the field and G is the height of the potential energy barrier. The equation in the left-hand panel assumes ion A to be present only on the outside, ion B only on the inside. For the two-barrier case, $n' \simeq 1 + \alpha_1^A - \alpha_2^B$ if G_1^A and G_2^B predominate for ions A and B, respectively. The bi-ionic n' is also affected by predominant barrier position asymmetry.

reaction rate theory predicts fluxes

$$m_e = \mathrm{B} f \frac{kT}{h} \exp[-G_1^{\mathrm{B}} - \alpha_1^{\mathrm{B}} \Psi + \Psi] \quad \text{(A1)}$$

$$m_i = \mathrm{A} f \frac{kT}{h} \exp[-G_1^{\mathrm{A}} - \alpha_1^{\mathrm{A}} \Psi] \quad \text{(A2)}$$

where f is the transmission coefficient (which we take to be the same for each ion) and k, T, and h have usual thermodynamic meanings. The ratio of the fluxes is

$$\frac{m_e}{m_i} = \frac{\mathrm{B}}{\mathrm{A}} \exp[-(G_1^{\mathrm{B}} - G_1^{\mathrm{A}}) + (1 + \alpha_1^{\mathrm{A}} - \alpha_1^{\mathrm{B}}) \Psi]. \quad \text{(A3)}$$

Solving for the reduced reversal potential (Ψ_{rev}) and substituting back in, this equation becomes

$$\frac{m_e}{m_i} = \exp[(1 + \alpha_1^{\mathrm{A}} - \alpha_1^{\mathrm{B}}) (\Psi - \Psi_{rev})]. \quad \text{(A4)}$$

The equation has a form similar to the modified Ussing flux ratio equation for a single species of ion

$$\frac{m_e}{m_i} = \exp[n'(\Psi - \Psi_{rev})]. \quad \text{(A5)}$$

It is clear that the bi-ionic flux ratio exponent, n', for this model is

$$n' = 1 + \alpha_1^A - \alpha_1^B. \quad \text{(A6)}$$

If the internal and external species were identical, the barrier would be at the same position in the field for both. Therefore, in this case $\alpha_1^A = \alpha_1^B$ and $n' = 1$, as it must for a single-barrier model with only one permeant ion. However, since in bi-ionic conditions the internal and external species are different, the barrier to the internal ion could be (considering an extreme case) at $\alpha_1^B = 1$ (the internal surface) and the external ion's barrier at $\alpha_1^A = 0$ (the external surface). Inserting these values of into Eqs. A1 and A2 we can see that in this case the flux ratio exponent would be 0. Because under these conditions unidirectional fluxes are independent of voltage, the ratio of fluxes is also independent of voltage. Similarly, with the internal ion's barrier at the external surface ($\alpha_1^B = 0$), and the external ion's barrier at the internal surface ($\alpha_1^A = 1$), $n' = 2$. Thus, for the bi-ionic situation in single-barrier pores, n' can differ from unity in either direction because of differences in the positions of the barriers for the two permeant species.

Without much difficulty this observation can be extended to more complicated pores. For instance a saturable pore might have two barriers, one of which predominates for each of the two ion species. This case is illustrated in the central panel of Fig. 9. For this case the flux ratio becomes

$$\frac{m_e}{m_i} = \frac{\mathrm{B}}{\mathrm{A}} \exp[-(G_2^{\mathrm{B}} - G_2^{\mathrm{A}}) - (G_1^{\mathrm{B}} - G_1^{\mathrm{A}}) + (1 + \alpha_1^{\mathrm{A}} - \alpha_1^{\mathrm{B}} + \alpha_2^{\mathrm{A}} - \alpha_2^{\mathrm{B}})\Psi] X, \quad \text{(A7)}$$

where

$$X = \frac{\exp(-G_1^{\mathrm{A}} - \alpha_1^{\mathrm{A}}\Psi) + \exp(-G_2^{\mathrm{A}} - \alpha_2^{\mathrm{A}}\Psi)}{\exp(-G_1^{\mathrm{B}} - \alpha_1^{\mathrm{B}}\Psi) + \exp(-G_2^{\mathrm{B}} - \alpha_2^{\mathrm{B}}\Psi)}. \quad \text{(A7a)}$$

Note that the well depths do not appear in this equation. If barrier 1 predominates for ion A ($G_1^A >> G_2^A$) and barrier 2 predominates for ion B ($G_2^B >> G_1^B$), the factor X approaches

$$X \simeq \frac{\exp(-G_2^{\mathrm{A}} - \alpha_2^{\mathrm{A}}\Psi)}{\exp(-G_1^{\mathrm{B}} - \alpha_1^{\mathrm{B}}\Psi)} \quad \text{(A8)}$$

for moderate values of Ψ. The flux ratio then becomes

$$\frac{m_e}{m_i} \simeq \frac{\mathrm{B}}{\mathrm{A}} \exp[-(G_2^{\mathrm{B}} - G_1^{\mathrm{A}}) + (1 + \alpha_1^{\mathrm{A}} + \alpha_2^{\mathrm{B}})\Psi], \quad \text{(A9)}$$

which is comparable to the single-barrier result in Eq. 7. The value of n' becomes

$$n' \simeq 1 + \alpha_1^A - \alpha_2^B. \quad \text{(A10)}$$

Thus, for the two-barrier model, if the positions of the predominating barriers differ, n' will deviate from unity by the difference between their fractional locations.

Another example which was convenient for us since well-tested programs for calculating the flux ratio were available was the three-barrier, two-site, multiple-occupancy model. This is illustrated in the right-hand panel of Fig. 9. Though the analytical solution for the flux ratio is complicated both by the increased number of barriers and by the possibility of multiple occupancy, one might expect the same qualitative result as for the one-barrier and two-barrier cases. Indeed, by making the inside barrier (at position α_3^B) high for the inside ion and the outside barrier (at position α_1^A) high for the outside ion and the others negligibly small, the calculated n' might be expected to be $1 + \alpha_1^A - \alpha_3^B$. The case we tried, $\alpha_1^A = 1/6$, $\alpha_3^B = 5/6$, gave $n' = 1/3$ between -100 and $+100$ mV. Therefore, even for the multiply occupied pore, n' values in bi-ionic conditions can primarily reflect differences in the positions of predominant barriers.

We thank E. Caufield of Arrive Alive Biological Supply Co. Long Island, N.Y. for supplying squid to Rochester and Lynette Morgan for typing the manuscript.

Financial support for this work was provided by U . S. Public Health Service grants NS-14138 and NS-00322. D. Busath was supported by National Research Service Award number NS-06084.

Received for publication 2 February 1982 and in revised form 10 May 1982.RM

REFERENCES

Armstrong, C. M. 1969. Inactivation of the potassium conductance and related phenomena caused by quaternary ammonium ion injection in squid axons. *J. Gen. Physiol.* 54:553–575.

Begenisich, T., and D. Busath. 1981. Sodium flux ratio in voltage-clamped squid giant axons. *J. Gen. Physiol.* 77:489–502.

Begenisich, T. B., and M. D. Cahalan. 1980 *a*. Sodium channel permeation in squid axons: I. Reversal potential experiments. *J. Physiol. (Lond.).* 307:217–242.

Begenisich, T. B., and M. D. Cahalan. 1980 *b*. Sodium channel permeation in squid axons: II. Non-independence and current-voltage relations. *J. Physiol. (Lond.).* 307:243–257.

Begenisich, T., and P. De Weer. 1976. Ionic interactions in the potassium channel of squid giant axons. *Nature (Lond.).* 769:710–711.

Begenisich, T., and P. De Weer. 1980. Potassium flux ratio in voltage-clamped squid giant axons. *J. Gen. Physiol.* 76:83–98.

Begenisich, T., and C. Lynch. 1974. Effects of internal divalent cations on voltage clamped squid axons. *J. Gen. Physiol.* 63:675–689.

Binstock, L., W. J. Adelman, Jr., J. P. Serft, and H. Lecar. 1975. Determination of the resistance in series with the membranes of giant axons. *J. Membr. Biol.* 21:25–47.

Heckman, K. 1972. Single file diffusion. *Biomembranes.* 3:127–153.

Hille, B. 1975. Ionic selectivity of Na and K channels of nerve membranes. *In* Membranes: A Series of Advances. G. Eisenman, editor. Marcel Dekker, Inc. New York. 3:255–323.

Hille, B., and W. Schwarz. 1978. Potassium channels as multi-ion singlefile pores. *J. Gen. Physiol.* 72:409–442.

Hodgkin, A. L., and R. D. Keynes. 1955. The potassium permeability of a giant nerve fibre. *J. Physiol.* (*Lond.*). 128:61–88.

Kirsch, G. E., and T. Narahashi. 1978. 3,4-Diaminopyridine—potent new potassium channel blocker. *Biophys. J.* 22:507–512.

Levis, R. 1981. Temporal control of potential in a giant axon voltage clamp. *Biophys. J.* 25:306*a*.

Salzberg, B., F. Bezanilla, and H. V. Davila. 1981. An optical determination of the series resistance in giant axons of *Loligo pealei*. *Biophys. J.* 33:90 *a*.

Taylor, R. E., C. M. Armstrong, and F. Bezanilla. 1976. Block of sodium channels by external calcium ions. *Biophys. J.* 16:27 *a*.

Ussing, H. H. 1949. The distinction by means of tracers between active transport and diffusion. *Acta Physiol. Scand.* 19:43–56.

Woodhull, A. M. 1973. Ionic blockage of sodium channels. *J. Gen. Physiol.* 61:687–708.